

From F Bassani; Giuseppe Pastori Parravicini; R A Ballinger,
Electronic states and optical transitions in solids, Franklin Book Co. 1993
(originally published in 1975)

CHAPTER 5

INTERBAND TRANSITIONS AND OPTICAL PROPERTIES

IN THIS chapter we wish to study the relationship between the electronic band structure and the optical properties in crystals. We shall confine ourselves here to the case of interband transitions. Emphasis will be given to the discussion of that part of the structure in the optical constants which may be understood on the basis of the symmetry properties of the crystal. We shall also discuss in detail a couple of particularly effective examples. A review of the experimental situation up to 1968 for the case of semiconductors can be found in the book by Greenaway and Harbeke.^[1] In the last few years new optical measurements have been accumulated for all types of solids and have been interpreted on the basis of the quantum theory of band-to-band transitions. The effect of exciton interaction on the optical spectrum will be discussed in the following chapter.

5-1 General theoretical analysis of band-to-band optical transitions^[2]

5-1 a Basic approximations

The effect of a radiation field on the crystal electronic states can be studied using standard quantum mechanical methods. From standard classical mechanics we know that the kinetic energy of a system of N electrons

$$\sum_{i=1}^N \frac{\mathbf{p}_i^2}{2m}$$

has to be replaced, in the presence of an electromagnetic field, by the expression

$$\sum_{i=1}^N \left[\frac{1}{2m} \left(\mathbf{p}_i + \frac{e\mathbf{A}(\mathbf{r}_i, t)}{c} \right)^2 \right],$$

where e is the absolute value of the electron charge, \mathbf{A} is the vector potential of the electromagnetic field, and the scalar potential V has been taken as zero without loss of generality because of the arbitrariness in the gauge. The Lorentz condition and the choice $V = 0$ imply $\nabla \cdot \mathbf{A} = 0$. Furthermore we can now neglect non-linear effects by disregarding the term in \mathbf{A}^2 . We then find that the interaction Hamiltonian of electrons in a radiation field is given by the expression

$$H_{eR} = \frac{e}{mc} \sum_{i=1}^N \mathbf{A}(\mathbf{r}_i, t) \cdot \mathbf{p}_i. \quad (5-1)$$

The effect of a radiation field on the crystal states can be studied by treating H_{eR} as a time dependent perturbation term on the electronic states of the crystal described in the previous chapters. This time dependent term will cause electrons to make transitions between occupied bands and empty bands. From the transition probability rate, the relationship between the electronic structure and the phenomenological optical constants can be derived.

We suppose that the electronic states are those computed in the adiabatic scheme and using the one-electron approximation (Section 3-1). Furthermore we make use of Koopmans' approximation (Appendix 5B), thus neglecting electron polarization effects. The above basic approximations must be taken as a starting point only in studying the optical properties of some crystals, and improvements leading to indirect transitions and exciton effects will be discussed in Section 5-4 and in Chapter 6.

5-1 b Quantum theory of band-to-band transitions

From elementary quantum mechanics we know that, to first order perturbation theory, the probability per unit time that a perturbation of the form $\mathcal{L}e^{\mp i\omega t}$ (where the time dependence is completely contained in $e^{\mp i\omega t}$) induces a transition from the initial state $|i\rangle$ of energy E_i to the final state $|f\rangle$ of energy E_f is

$$\mathcal{P}_{i \rightarrow f} = \frac{2\pi}{\hbar} |\langle f | \mathcal{L} | i \rangle|^2 \delta(E_f - E_i \mp \hbar\omega). \quad (5-2)$$

The above relation has the interpretation that a perturbation $\mathcal{L}e^{-i\omega t}$ induces transitions with absorption of a quantum $\hbar\omega$, while a perturbation $\mathcal{L}e^{i\omega t}$ gives rise to emission of a quantum $\hbar\omega$. Since the perturbation must be real we have the sum of both absorption and emission terms, but the choice of initial and final states in (5-2) selects out the term to be considered. If the initial state is the ground state, the emission term makes expression (5-2) vanish. Thus only the absorption term needs to be considered in discussing the optical excitation spectrum of a crystal in the ground state. The emission term in (5-2) is relevant in discussing the radiative emission due to electrons initially in excited states (luminescence, phosphorescence, and pair recombination at impurity centres). We will neglect the emission term in the present treatment, keeping in mind that it could be dealt with, when needed, just by putting the appropriate sign into the argument of the δ function.

To second order, the transition probability rate is

$$\mathcal{P}_{i \rightarrow f} = \frac{2\pi}{\hbar} \left| \sum_{\beta} \frac{\langle f | \mathcal{L} | \beta \rangle \langle \beta | \mathcal{L} | i \rangle}{E_{\beta} - E_i \mp \hbar\omega} \right|^2 \delta(E_f - E_i \mp \hbar\omega \mp \hbar\omega), \quad (5-3)$$

where $|\beta\rangle$ indicates all intermediate states including initial and final state. The matrix elements appearing in (5-3) can be regarded as a result of two successive processes—firstly, the system makes a transition from the state $|i\rangle$ to the state $|\beta\rangle$, and, secondly, from $|\beta\rangle$ to $|f\rangle$. Energy is not conserved in the intermediate transition; it is only conserved between initial and final states. Also in this case the considerations made before about absorption and emission processes apply.

In a similar way we can extend the computation of the transition probability rate to higher order as an obvious generalization of (5-2) and (5-3). We must keep in mind that the argument of the δ function is $E_f - E_i \mp \hbar\omega \cdots \mp \hbar\omega$, where the number of

quanta absorbed or emitted gives the order of the transition, and the matrix elements connecting the initial and the final state through different intermediate states are divided by energy differences which include an appropriate number of quanta $\hbar\omega$. To third order we obtain, for example,

$$\mathcal{P}_{i \rightarrow f} = \frac{2\pi}{\hbar} \left| \sum_{\alpha\beta} \frac{\langle f | \mathcal{L} | \alpha \rangle \langle \alpha | \mathcal{L} | \beta \rangle \langle \beta | \mathcal{L} | i \rangle}{(E_\alpha - E_i \mp \hbar\omega \mp \hbar\omega)(E_\beta - E_i \mp \hbar\omega)} \right|^2 \delta(E_f - E_i \mp \hbar\omega \mp \hbar\omega \mp \hbar\omega).$$

We will be mostly interested in first order transitions of type (5-2), but will also discuss effects due to higher order terms in Sections 5-3 and 5-4.

The interaction of a radiation field with the electronic states of a crystal may induce both interband and intraband transitions. In semiconductors (and insulators) the ground state of the whole crystal at zero absolute temperature, contains completely occupied or completely empty bands, and as a consequence only interband transitions need be considered. For semiconductors at finite temperatures and also for metals there is also a free carrier absorption for long wavelength radiation (in general, in the infrared region), but we will not consider the optical absorption by free carriers here although it is worth while to point out that its theory is quite similar to that of interband transitions.

We now calculate the contribution to the optical constants due to a couple of valence and conduction bands. For simplicity we make the further assumption of neglecting relativistic effects, an approximation which could easily be removed if required. The ground state of the electronic system can be written (in the adiabatic and one-electron approximation) as a Slater determinant

$$\Psi_0 = \mathcal{A} \{ \psi_{v_{k_1}}(\mathbf{r}_1) \alpha(1) \psi_{v_{k_2}}(\mathbf{r}_2) \beta(2) \dots \psi_{v_{k_{s_i}}(\mathbf{r}_n)} \dots \psi_{v_{k_N}}(\mathbf{r}_{2N}) \beta(2N) \},$$

where \mathcal{A} is the antisymmetrizing operator, N is the number of unit cells, v refers to a specific valence band, α and β are the spin eigenfunctions, and s_i is a spin index indicating either α or β . A trial excited state, in which the conduction wave function $\psi_{c_{k_f s_f}}$ replaces the valence wave function $\psi_{v_{k_i s_i}}$ can be written as

$$\Psi' = \mathcal{A} \{ \psi_{v_{k_1}}(\mathbf{r}_1) \alpha(1) \psi_{v_{k_2}}(\mathbf{r}_2) \beta(2) \dots \psi_{c_{k_f s_f}}(\mathbf{r}_n) \dots \psi_{v_{k_N}}(\mathbf{r}_{2N}) \beta(2N) \}.$$

We need the matrix elements of the operator H_{eR} [defined in (5-1)] between the ground state and the excited states. Since H_{eR} is a sum of one-particle operators, the non-vanishing matrix elements connect the ground state Ψ_0 with states Ψ' having only one electron which is excited. This is shown explicitly in Appendix 5A; from formula (5A-3) we can write

$$\begin{aligned} \langle \Psi' | H_{eR} | \Psi_0 \rangle &= \frac{e}{mc} \langle \psi_{c_{k_f s_f}} | \mathbf{A} \cdot \mathbf{p} | \psi_{v_{k_i s_i}} \rangle \\ &= \frac{e}{mc} \delta_{s_i, s_f} \langle \psi_{c_{k_f}} | \mathbf{A} \cdot \mathbf{p} | \psi_{v_{k_i}} \rangle. \end{aligned}$$

For radiation of a given frequency ω the vector potential \mathbf{A} can be written as

$$\mathbf{A}(\mathbf{r}, t) = A_0 \mathbf{e} e^{i(\boldsymbol{\eta} \cdot \mathbf{r} - \omega t)} + \text{c.c.}, \quad (5-4)$$

where \mathbf{e} is the polarization vector in the direction of the electric field, $\boldsymbol{\eta}$ is the wave vector of the radiation, and c.c. indicates the complex conjugate of the previous term.

We shall only consider the effect of the first term in (5-4) which gives rise to the absorption.

The transition probability per unit time (5-2) now becomes

$$\mathcal{P}_{v\mathbf{k}_i s_i \rightarrow c\mathbf{k}_f s_f} = \frac{2\pi}{\hbar} \left(\frac{eA_0}{mc} \right)^2 \delta_{s_i, s_f} |\langle \psi_{c\mathbf{k}_f} | e^{i\boldsymbol{\eta} \cdot \mathbf{r}} \mathbf{e} \cdot \mathbf{p} | \psi_{v\mathbf{k}_i} \rangle|^2 \delta(E_f - E_i - \hbar\omega), \quad (5-5)$$

which is the basic expression for computing optical constants in the frequency region of interband transitions.

Let us now consider the matrix element

$$\langle \psi_{c\mathbf{k}_f} | e^{i\boldsymbol{\eta} \cdot \mathbf{r}} \mathbf{e} \cdot \mathbf{p} | \psi_{v\mathbf{k}_i} \rangle. \quad (5-6)$$

The function $\psi_{c\mathbf{k}_f}$ belongs to the irreducible representation of the translation group with vector \mathbf{k}_f . The function $\psi_{v\mathbf{k}_i}$, as well as its derivative $\mathbf{e} \cdot \mathbf{p} \psi_{v\mathbf{k}_i}$, belongs to the irreducible representation with vector \mathbf{k}_i , and $e^{i\boldsymbol{\eta} \cdot \mathbf{r}}$ belongs to the irreducible representation of vector $\boldsymbol{\eta}$. Since the product of the irreducible representation \mathbf{k}_i by the irreducible representation $\boldsymbol{\eta}$ is the irreducible representation $\mathbf{k}_i + \boldsymbol{\eta}$, selection rules of the type discussed in Section 2-4b result. Thus the matrix element (5-6) is zero unless

$$\mathbf{k}_f = \mathbf{k}_i + \boldsymbol{\eta} + \mathbf{h}, \quad (5-7)$$

\mathbf{h} being any reciprocal lattice vector. The above equation expresses the conservation of momentum in a periodic medium. We observe that for typical photon energies of the order of an electron volt, the wavelength is of the order of 10^4 \AA and

$$|\boldsymbol{\eta}| \approx 2\pi/10^4 \text{ \AA}^{-1}.$$

The range of variation of \mathbf{k}_i (and \mathbf{k}_f) is $2\pi/a$ with a of the order of a few angstroms. The wave functions and energies in a given band are functions which depend slowly on \mathbf{k} (compared with variations of the order of $\boldsymbol{\eta}$), and so for all practical purposes we can neglect the radiation propagation vector $\boldsymbol{\eta}$ in eq. (5-6). Furthermore, since \mathbf{k}_i and \mathbf{k}_f are confined to the first Brillouin zone, we may write

$$\mathbf{k}_i \simeq \mathbf{k}_f. \quad (5-8)$$

We thus arrive at the result that only "vertical" transitions can be induced in an energy band diagram by the radiation field (Fig. 5-1). Equation (5-7) expresses the conservation of momentum in crystals and (5-8) is the dipole approximation. We can therefore simplify the expression for the probability per unit time given in (5-5) as

$$\mathcal{P}_{v\mathbf{k}s \rightarrow c\mathbf{k}s} = \frac{2\pi}{\hbar} \left(\frac{eA_0}{mc} \right)^2 |\mathbf{e} \cdot \mathbf{M}_{cv}(\mathbf{k})|^2 \delta(E_c(\mathbf{k}) - E_v(\mathbf{k}) - \hbar\omega), \quad (5-9a)$$

where

$$\begin{aligned} \mathbf{e} \cdot \mathbf{M}_{cv}(\mathbf{k}) &= \langle \psi_{c\mathbf{k}} | \mathbf{e} \cdot \mathbf{p} | \psi_{v\mathbf{k}} \rangle \\ &= \mathbf{e} \cdot \int_{\text{crystal volume}} \psi_c^*(\mathbf{k}, \mathbf{r}) (-i\hbar \nabla) \psi_v(\mathbf{k}, \mathbf{r}) d\mathbf{r}. \end{aligned} \quad (5-9b)$$

To obtain the number of transitions $W(\omega)$ per unit time per unit volume induced by light of frequency ω , we must sum (5-9a) over all possible states in the unit volume, i.e. we must sum over \mathbf{k} , the spin variable s , and over the band indices v (occupied)

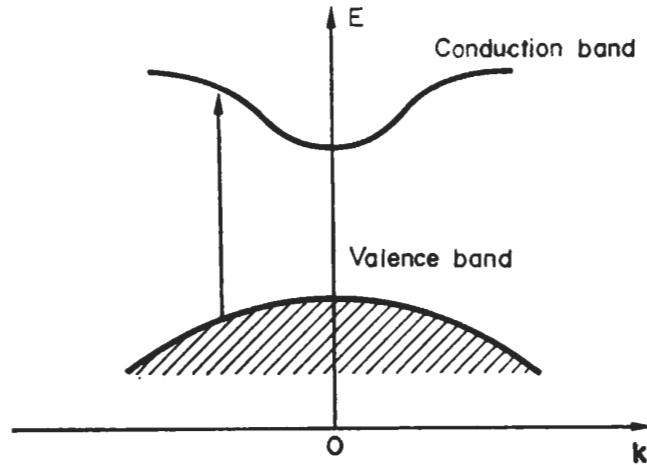


FIG. 5-1. Schematic representation in an energy band diagram of vertical transitions produced by a radiation field.

and c (empty). Since the allowed \mathbf{k} vectors are distributed in the Brillouin zone with a density $V/(2\pi)^3$ (V being the crystal volume),

$$W(\omega) = \frac{2\pi}{\hbar} \left(\frac{eA_0}{mc} \right)^2 \sum_{v,c} \int_{\text{BZ}} \frac{2d\mathbf{k}}{(2\pi)^3} |\mathbf{e} \cdot \mathbf{M}_{cv}(\mathbf{k})|^2 \delta(E_c(\mathbf{k}) - E_v(\mathbf{k}) - \hbar\omega), \quad (5-10)$$

where the integral extends over the first Brillouin zone and the factor of 2 arises from the integration of spin variables.

5-1 c Connection with the optical constants^[1-3]

We wish now to derive the relation between expression (5-10) and the optical constants which are used phenomenologically to describe the optical properties of matter. Optical properties can be described in terms of the complex dielectric function $\epsilon = \epsilon_1 + i\epsilon_2$ or the complex refractive index $N = n + ik$, where n is the ordinary refractive index and k is known as the extinction coefficient. The optical constants ϵ and N are connected by the relation $\epsilon = N^2$, and the absorption coefficient α depends on the above optical constants via

$$\alpha = \frac{2k\omega}{c}, \quad (5-11)$$

$$\alpha = \frac{\omega}{nc} \epsilon_2. \quad (5-12)$$

The average energy density u in a medium of a radiation field described by the vector potential (5-4) is related to the optical constants through the relation

$$u = \frac{n^2 A_0^2 \omega^2}{2\pi c^2}.$$

It is also known that the radiation in the medium propagates with velocity c/n . Using (5-10) we can now obtain microscopic expressions for the absorption coefficient and

the other optical constants. The absorption coefficient is by definition the energy absorbed in the unit time in the unit volume divided by the energy flux

$$\alpha(\omega) = \frac{\hbar\omega W(\omega)}{u(c/n)},$$

where $\hbar\omega W(\omega)$ is the energy absorbed per unit volume and time, and the product $u(c/n)$ of the energy density by the velocity of propagation in the medium is the energy flux. We thus obtain for the absorption coefficient

$$\alpha(\omega) = \frac{4\pi^2 e^2}{ncm^2\omega} \sum_{v,c} \int_{\text{BZ}} \frac{2d\mathbf{k}}{(2\pi)^3} |\mathbf{e} \cdot \mathbf{M}_{cv}(\mathbf{k})|^2 \delta(E_c(\mathbf{k}) - E_v(\mathbf{k}) - \hbar\omega). \quad (5-13)$$

Using (5-12)

$$\varepsilon_2(\omega) = \frac{4\pi^2 e^2}{m^2\omega^2} \sum_{v,c} \int_{\text{BZ}} \frac{2d\mathbf{k}}{(2\pi)^3} |\mathbf{e} \cdot \mathbf{M}_{cv}(\mathbf{k})|^2 \delta(E_c(\mathbf{k}) - E_v(\mathbf{k}) - \hbar\omega). \quad (5-14)$$

This is the basic expression which connects the band structure with the optical properties; it is preferred over related expressions for other optical constants because it does not depend on the refractive index.

The quantum expression for $\varepsilon_1(\omega)$ can be obtained using the dispersion relation of Kramers-Kronig^[3]

$$\varepsilon_1(\omega) = 1 + \frac{2}{\pi} P \int_0^\infty \omega' \varepsilon_2(\omega') \frac{1}{\omega'^2 - \omega^2} d\omega', \quad (5-15)$$

where P indicates the principal part. By direct substitution of (5-14) into (5-15),

$$\varepsilon_1(\omega) = 1 + \frac{8\pi e^2}{m^2} \sum_{v,c} \int_{\text{BZ}} \frac{2d\mathbf{k}}{(2\pi)^3} \frac{|\mathbf{e} \cdot \mathbf{M}_{cv}(\mathbf{k})|^2}{[E_c(\mathbf{k}) - E_v(\mathbf{k})]/\hbar} \frac{1}{[E_c(\mathbf{k}) - E_v(\mathbf{k})]^2/\hbar^2 - \omega^2}. \quad (5-16)$$

?

The relations (5-14) and (5-16) allow in principle the computation of all optical constants once the band structure is known.

The optical constants satisfy some general relations which are often used to test the consistency of the approximations involved in their computation.^[3,4] A very useful relation is the sum rule

$$\int_0^\infty \omega \varepsilon_2(\omega) d\omega = \frac{\pi}{2} \omega_p^2, \quad (5-17a)$$

where the plasma frequency ω_p is given by

$$\omega_p = \left(\frac{4\pi n e^2}{m} \right)^{1/2} \quad (5-17b)$$

and n denotes the density of the electrons which take part in the transition. Another useful sum rule is obtained as a particular case of the dispersion relation (5-15), taking the limit $\omega \rightarrow 0$.

$$\varepsilon_1(0) = 1 + \frac{2}{\pi} \int_0^\infty \frac{\varepsilon_2(\omega)}{\omega} d\omega. \quad (5-18)$$

Two particularly important sum rules on the index of refraction for isotropic media are

$$\int_0^{\infty} [n(\omega) - 1] d\omega = 0 \quad (5-19)$$

and

$$\int_0^{\infty} \omega k(\omega) d\omega = \frac{\pi}{4} \omega_p^2. \quad (5-20)$$

5-2 Structure of the optical constants at critical points

5-2a Theoretical discussion

The standard procedure for obtaining theoretically the optical constants of a crystal is to evaluate expression (5-14) for the imaginary part of the dielectric function. We shall now discuss in some detail specific cases and will show that a structure in the optical constants results with peaks at critical points.

The matrix elements $|\mathbf{e} \cdot \mathbf{M}_{cv}(\mathbf{k})|^2$ between a given couple of valence and conduction bands are shown to be (see Section 3-9) smooth functions of \mathbf{k} , except near special \mathbf{k} vectors where $\mathbf{e} \cdot \mathbf{M}_{cv}(\mathbf{k})$ vanishes because of symmetry. Neglecting such a situation and taking $\mathbf{e} \cdot \mathbf{M}_{cv}(\mathbf{k})$ as a constant, we find from eq. (5-14) that the contribution to the dielectric function from a pair of bands is proportional to $1/\omega^2$ and to the quantity

$$J_{cv}(\hbar\omega) = \int_{\text{BZ}} \frac{2d\mathbf{k}}{(2\pi)^3} \delta[E_c(\mathbf{k}) - E_v(\mathbf{k}) - \hbar\omega], \quad (5-21)$$

which is called joint density of states because it gives the density of pair of states—one occupied and the other empty—separated by an energy $\hbar\omega$.

The integration in (5-21) can be performed by using the properties of the δ function. We know that

$$\int_a^b g(x) \delta[f(x)] dx = \sum_{x_0} g(x_0) \left| \frac{df}{dx} \right|_{x=x_0}^{-1}, \quad (5-22)$$

in which x_0 represents a zero of the function $f(x)$ contained in the interval (a, b) . In three dimensions

$$J_{cv}(E) = \frac{2}{(2\pi)^3} \int_{E_c(\mathbf{k}) - E_v(\mathbf{k}) = E} \frac{dS}{|\nabla_{\mathbf{k}}[E_c(\mathbf{k}) - E_v(\mathbf{k})]|}, \quad (5-23)$$

where dS represents an element of surface in \mathbf{k} space on the surface defined by the equation

$$E_c(\mathbf{k}) - E_v(\mathbf{k}) = E.$$

The joint density of states for interband transitions as a function of E shows strong variations in the neighbourhood of particular values of E which are called critical point energies. From eq. (5-23) we see that singularities in the joint density of states are expected when

$$\nabla_{\mathbf{k}} E_c(\mathbf{k}) = \nabla_{\mathbf{k}} E_v(\mathbf{k}) = 0, \quad (5-24a)$$

or more generally when

$$\nabla_{\mathbf{k}} E_c(\mathbf{k}) - \nabla_{\mathbf{k}} E_v(\mathbf{k}) = 0. \quad (5-24b)$$

Critical points of type (5-24a) occur in general at high symmetry points of the Brillouin zone, while critical points of type (5-24b) may occur at any \mathbf{k} vector. The number of critical points which may occur in the Brillouin zone has been discussed by Phillips,^[5] and the types of singularity have been analysed by Van Hove.^[5]

The analytic behaviour of $J_{cv}(E)$ near a singularity may be found by expanding $E_c(\mathbf{k}) - E_v(\mathbf{k})$ in a Taylor series about the critical point. In the expansion, linear terms do not occur because of conditions (5-24). Limiting the expansion to quadratic terms and denoting the wave vectors along the principal axes with the origin at the critical point by k_x, k_y, k_z ,

$$E_c(\mathbf{k}) - E_v(\mathbf{k}) = E_0 + \frac{\hbar^2}{2} \left(\varepsilon_x \frac{k_x^2}{m_x} + \varepsilon_y \frac{k_y^2}{m_y} + \varepsilon_z \frac{k_z^2}{m_z} \right), \quad (5-25)$$

with m_x, m_y, m_z positive quantities and $\varepsilon_x, \varepsilon_y, \varepsilon_z$ equal to $+1$ or -1 . We obtain four types of singularities, depending on the signs of $\varepsilon_x, \varepsilon_y, \varepsilon_z$. The critical points are called:

- M_0 when all coefficients of the quadratic expansion are positive (minimum);
- M_1 when two coefficients are positive and one negative (saddle point);
- M_2 when two coefficients are negative and one positive (saddle point);
- M_3 when all coefficients are negative (maximum),

where the subscripts attached to M indicate the number of negative coefficients in the expansion of the energy differences.

The analytic behaviour of the joint density of states near critical points can be obtained using (5-21) and (5-25). We report the results in Table 5-1, and we notice that there are sharp discontinuities at the critical points.

Proof. As an illustration of the results reported in Table 5-1, let us consider the case of the point M_1 .

In the expansion (5-25) we have $\varepsilon_x = \varepsilon_y = 1$ and $\varepsilon_z = -1$, and substituting in (5-21)

$$J_{cv}(E) = \int_{\text{BZ}} \frac{2d\mathbf{k}}{(2\pi)^3} \delta \left(E_0 + \frac{\hbar^2}{2} \frac{k_x^2}{m_x} + \frac{\hbar^2}{2} \frac{k_y^2}{m_y} - \frac{\hbar^2}{2} \frac{k_z^2}{m_z} - E \right).$$

We introduce the new coordinates

$$q_i = \frac{\hbar}{(2m_i)^{1/2}} k_i \quad (i = x, y, z)$$

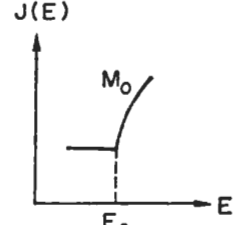

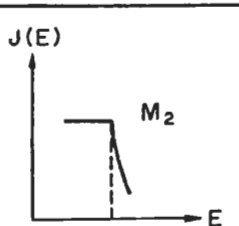
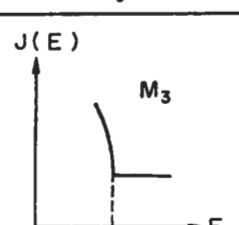
and obtain

$$J_{cv}(E) = \frac{2}{(2\pi)^3} \frac{2^{3/2}(m_x m_y m_z)^{1/2}}{\hbar^3} \int d\mathbf{q} \delta(E_0 + q_x^2 + q_y^2 - q_z^2 - E).$$

Using cylindrical coordinates q, φ in the (q_x, q_y) plane, we transform the above equation into

$$J_{cv}(E) = \frac{2}{(2\pi)^3} \frac{2^{3/2}(m_x m_y m_z)^{1/2}}{\hbar^3} 2\pi \iint q dq dq_z \delta(q^2 - q_z^2 + E_0 - E).$$

TABLE 5-1. Analytic behaviour and schematic representation of the joint density of states near critical points for the three-dimensional case. For convenience $A = \pi 2^{7/2} \hbar^{-3} (m_x m_y m_z)^{1/2}$ and B indicates a constant which depends on the detailed band structure

Critical Point	Joint density of states	Schematic representation
M_0 Minimum	$J(E) = \begin{cases} B + O(E - E_0) & \text{when } E < E_0 \\ B + A(E - E_0)^{1/2} + O(E - E_0) & \text{when } E > E_0 \end{cases}$	
M_1 Saddle point	$J(E) = \begin{cases} B - A(E_0 - E)^{1/2} + O(E - E_0) & \text{when } E < E_0 \\ B + O(E - E_0) & \text{when } E > E_0 \end{cases}$	
M_2 Saddle Point	$J(E) = \begin{cases} B + O(E - E_0) & \text{when } E < E_0 \\ B - A(E - E_0)^{1/2} + O(E - E_0) & \text{when } E > E_0 \end{cases}$	
M_3 Maximum	$J(E) = \begin{cases} B + A(E_0 - E)^{1/2} + O(E - E_0) & \text{when } E < E_0 \\ B + O(E - E_0) & \text{when } E > E_0 \end{cases}$	

Using (5-22) we can integrate with respect to q_z and obtain

$$J_{cv}(E) = \frac{2}{(2\pi)^2} \frac{2^{3/2} (m_x m_y m_z)^{1/2}}{\hbar^3} \int_0^R q \, dq \sum_{q_{z0}} \frac{1}{2|q_{z0}|}, \quad (5-26)$$

with

$$q_{z0} = \mp \sqrt{(q^2 + E_0 - E)} \quad \text{if } q^2 + E_0 - E > 0.$$

The above integration has been extended to a region surrounding the critical point; for convenience we have used a sphere of radius R in which the expansion holds. With the help of the step function

$$\eta(x) = \begin{cases} 1 & \text{for } x > 0, \\ 0 & \text{for } x < 0, \end{cases}$$

eq. (5-26) can be written as

$$J_{cv}(E) = A \int_0^R \frac{q dq}{\sqrt{(q^2 + E_0 - E)}} \eta(q^2 + E_0 - E)$$

where $A = \pi 2^{7/2} \hbar^{-3} (m_x m_y m_z)^{1/2}$.

If

$$E < E_0, \quad \eta(q^2 + E_0 - E) = 1,$$

$$\begin{aligned} J_{cv}(E) &= A \int_0^R \frac{q dq}{\sqrt{(q^2 + E_0 - E)}} = A(\sqrt{(E_0 - E + R^2)} - \sqrt{(E_0 - E)}) \\ &= -A\sqrt{(E_0 - E)} + O(E_0 - E), \end{aligned} \quad (5-27a)$$

where the last step is possible for an energy value E sufficiently near to the critical point energy E_0 so that $|E - E_0| \ll R^2$. The expression $O(E_0 - E)$ indicates a quantity that vanishes at least linearly when $E \rightarrow E_0$.

If $E > E_0$, then $\eta(q^2 + E_0 - E) = 1$ only if $q > \sqrt{(E - E_0)}$. Thus

$$J_{cv}(E) = A \int_{\sqrt{(E-E_0)}}^R \frac{q dq}{\sqrt{(q^2 + E_0 - E)}} = A\sqrt{(E_0 - E + R^2)} = O(E_0 - E). \quad (5-27b)$$

Expressions (5-27a) and (5-27b) represent the contribution to the joint density of states from a region surrounding the critical point. The contribution to $J_{cv}(E)$ from the remaining region of the Brillouin zone is a continuous quantity (provided that the other critical points are dealt with separately) which is taken into account by the smoothly energy dependent expression $O(E - E_0)$ of Table 5-1.

To complete our discussion of the joint density of states let us consider critical points in two-dimensional and one-dimensional structures. For crystals, in which the energy depends only on two components of \mathbf{k} , say k_x and k_y , the expression (5-21) for the joint density of states becomes

$$J_{cv}(E) = \frac{2\pi}{c} \int_{\text{BZ}} \frac{2}{(2\pi)^3} dk_x dk_y \delta(E_c(k_x, k_y) - E_v(k_x, k_y) - E), \quad (5-28)$$

where $2\pi/c$ appears because of the k_z integration, and BZ now indicates the two-dimensional Brillouin zone. Near a critical point, we can expand $E_c(k_x, k_y) - E_v(k_x, k_y)$ in the form

$$E_c(k_x, k_y) - E_v(k_x, k_y) = E_0 + \frac{\hbar^2}{2} \left(\epsilon_x \frac{k_x^2}{m_x} + \epsilon_y \frac{k_y^2}{m_y} \right).$$

We have in this case three types of critical points which we denote by P_0, P_1, P_2 , with subscripts indicating the number of coefficients which are negative. The method of calculation of the joint density of states is the same as that explained for the three-

dimensional case. At the points P_0 and P_2 a step function singularity occurs, while at the saddle point P_1 we have a logarithmic singularity. The results are given in Table 5-2.

For crystals, in which the energy depends only on one component of \mathbf{k} , say k_x , the expression (5-21) for the joint density of states becomes

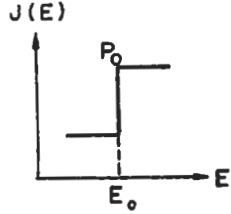
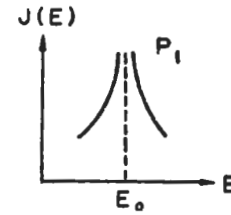
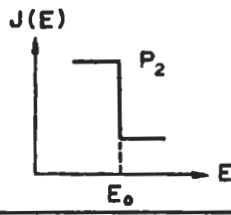
$$J_{cv}(E) = \frac{4\pi^2}{ab} \int_{BZ} \frac{2}{(2\pi)^3} dk_x \delta(E_c(k_x) - E_v(k_x) - E),$$

where $4\pi^2/ab$ appears because of the k_x, k_y integrations, and BZ now indicates the one-dimensional Brillouin zone. Two different critical points are obtained that we denote by Q_0 and Q_1 . The expression for the joint density of states can be immediately obtained using (5-22) and is given in Table 5-3.

We should like to point out at this juncture that changing the dimension of the \mathbf{k} vector has a profound effect on the nature of the singularities at the critical point. In the three-dimensional case we have basically shoulders and beak points, as can be seen from Table 5-1, while in the two-dimensional case we have a logarithmic singularity for a saddle point, and in the one-dimensional case we have sharp singularities of the type $(E - E_0)^{-1/2}$.

The results obtained from the theory of direct transitions can be compared with experimental results. For theoretical reasons (electron-electron, electron-lattice interaction, presence of imperfections) the singularities in the joint density of states are expected to be smoothed out in practice and to appear as peaks in the optical constants observed experimentally. We also expect the peaks in the two-dimensional case for the

TABLE 5-2. Analytic behaviour and schematic representation of the joint density of states near critical points for the two-dimensional case. For convenience $A = (8\pi/c) \hbar^{-2} (m_x m_y)^{1/2}$, and B indicates a constant which depends on the detailed band structure

Critical Point	Joint density of states	Schematic representation
P_0 Minimum	$J(E) = \begin{cases} B + O(E - E_0) & \text{when } E < E_0 \\ B + A + O(E - E_0) & \text{when } E > E_0 \end{cases}$	
P_1 Saddle point	$J(E) = B - \frac{A}{\pi} \ln \left 1 - \frac{E}{E_0} \right + O(E - E_0)$	
P_2 Maximum	$J(E) = \begin{cases} B + A + O(E - E_0) & \text{when } E < E_0 \\ B + O(E - E_0) & \text{when } E > E_0 \end{cases}$	

ELECTRONIC STATES AND OPTICAL TRANSITIONS

TABLE 5-3. Analytic behavior and schematic representation of the joint density of states near critical points for the one-dimensional case. For convenience $A = (4\pi/ab) \hbar^{-1} m_z^{1/2}$, and B indicates a constant which depends on the detailed band structure

Critical Point	Joint density of states	Schematic representation
Q_0 Minimum	$J(E) = \begin{cases} B + O(E - E_0) & \text{when } E < E_0 \\ B + A(E - E_0)^{-1/2} + O(E - E_0) & \text{when } E > E_0 \end{cases}$	
Q_1 Maximum	$J(E) = \begin{cases} B + A(E_0 - E)^{-1/2} + O(E - E_0) & \text{when } E < E_0 \\ B + O(E - E_0) & \text{when } E > E_0 \end{cases}$	

saddle point to be more easily detected than those in the three-dimensional case because of the sharpness of the logarithmic singularity. In the one-dimensional case they can be detected even better, as we will see in Chapter 8 in discussing the Landau levels.

We have so far considered the case of allowed transitions for which the structure in the dielectric function is basically determined by the joint density of states. The case of forbidden transitions is of no interest for M_1 , M_2 , or M_3 singularities because allowed transitions of equal energy occur in other regions of the Brillouin zone. In case the transition is forbidden at the edge the matrix element (5-9b) is proportional to $(\mathbf{k} - \mathbf{k}_0)$, and this dependence must be taken into account in carrying out the integration (5-14). The integral can be performed explicitly using (5-22), and one finds that the behaviour above the absorption edge is in this case $(E - E_0)^{3/2}$ instead of $(E - E_0)^{1/2}$ given in Table 5-1. We shall come back to this point in Chapter 6 when discussing the absorption edge including exciton effects.

5-2b Experimental evidence. Two examples: germanium and graphite

The basic features of the optical excitation spectra of many crystals can be explained on the basis of the analysis of Section 5-2a. The first quantitative success was obtained when the optical excitation spectrum of germanium was interpreted.^[6]

The calculation was performed numerically by sampling the Brillouin zone with a large number of points and computing the energy levels of valence and conduction bands at every \mathbf{k} point with the semi-empirical pseudopotential procedure which was discussed in Section 3-4b and whose application to the case of groups IV and III-V compounds was described in Section 4-1. Once the energy bands are computed at a large number of \mathbf{k} values (about one thousand independent points in germanium), one can see how many times a given energy difference occurs at all possible equally spaced values

of \mathbf{k} , thus numerically computing the joint density of states (5-21) for all couples of valence and conduction bands. The accuracy of the results depends on the number of points in \mathbf{k} space, and, furthermore, an energy difference must be considered equal to another if they differ by less than a fixed energy ΔE . The value of ΔE can be made smaller as the number of \mathbf{k} points in the sampling increases, but one must have a large number of points within any energy difference ΔE in order to avoid casual scattering. To obtain $\epsilon_2(\omega)$ the joint density of states is divided by ω^2 as indicated by (5-14) and multiplied by a constant which depends on the matrix element (5-9b) so as to satisfy the sum rule (5-17). The calculated dielectric function $\epsilon_2(\omega)$ so obtained is compared with the experimental curve in Fig. 5-2.

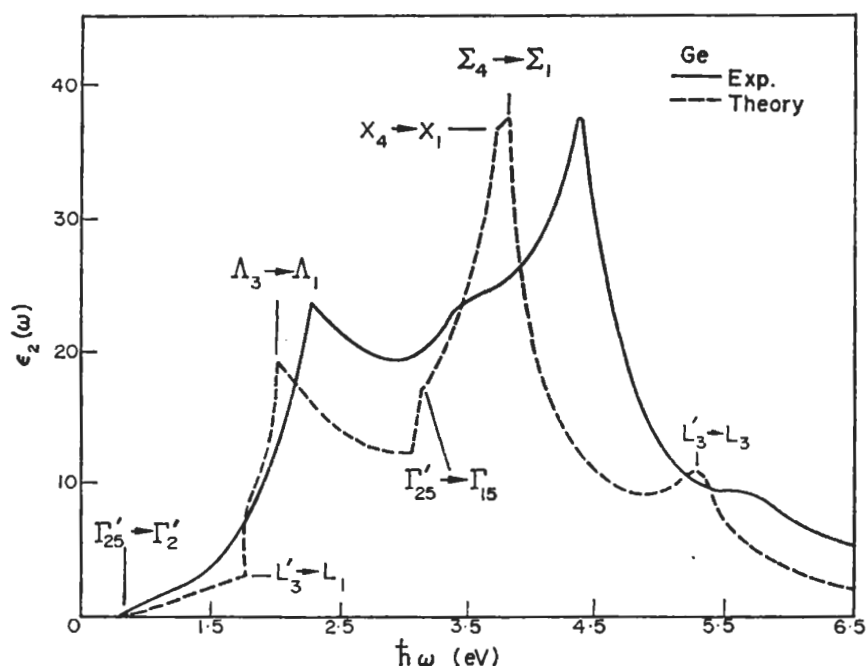


FIG. 5-2. Optical excitation spectrum of germanium shown by its $\epsilon_2(\omega)$ structure. The solid line gives the experimental results and the dashed line the theoretical results. The optical transitions at critical points are explicitly indicated. (From Brust *et al.*, ref. [6].)

It can be seen that the optical excitation spectrum from the direct edge at ≈ 0.8 eV to ≈ 7 eV is well interpreted by transitions from the highest valence band $L'_3 - \Gamma'_{25} - X_4$ to the two lowest conduction bands. It can be observed that the shoulders and peaks in the density of states at critical points are clearly present in the experimental spectrum. There is a shoulder corresponding to the transition $\Gamma'_{25} \rightarrow \Gamma'_2$ and a higher one corresponding to $\Gamma'_{25} \rightarrow \Gamma_{15}$; the shoulder at $L'_3 \rightarrow L_1$ is followed by a peak corresponding to the transition $\Lambda_3 \rightarrow \Lambda_1$ somewhere in the Λ direction; the sharp peak at about 3.5 eV is due to transitions at a number of points nearly degenerate, with a predominant contribution due to $X_4 \rightarrow X_1$. Further confirmation of this interpretation was obtained by the observation of the spin-orbit splittings associated to the states of the valence band Γ'_{25} , L'_3 , and Λ_3 in the corresponding transitions, and by many other properties of the transitions in the presence of external perturbations which will be discussed in Chapter 8.

After the success obtained with germanium, this same analysis was carried out also for silicon, for a large number of III-V compounds and many other crystals;

we may recognize that it has now become almost a standard procedure. For a detailed critical review of the experimental determination of the optical constants in a large number of semiconductors and of their interpretation in terms of interband transitions, we refer to the book by Greenaway and Harbeke.^[1]

As a second example we shall consider the optical excitation spectrum of graphite in order to show new effects due to the strong anisotropy in the optical constants. The electronic band structure of graphite has been discussed in Section 4-2, where we have shown that for this layer crystal the two-dimensional approximation to the band structure gives meaningful results, and the interlayer interaction can be treated as a small perturbation. From (5-14), neglecting the small k_z dependence of the energy,

$$\epsilon_2(\omega) = \frac{2e^2}{cm^2\omega^2} \int_{\text{BZ}} |\mathbf{e} \cdot \mathbf{M}_{cv}(\mathbf{k})|^2 \delta(E_c(k_x, k_y) - E_v(k_x, k_y) - \hbar\omega) dk_x dk_y, \quad (5-29)$$

where c is the periodicity in the z direction, and BZ is the Brillouin zone of Fig. 4-10. From the energy band diagram of Fig. 4-11 we see that the only possible transitions with energy up to $\simeq 6$ eV occur between π bands, provided that $\mathbf{e} \cdot \mathbf{M}_{cv}(\mathbf{k})$ does not vanish. When \mathbf{e} is parallel to the z axis, the matrix element $\mathbf{e}_{\parallel} \cdot \mathbf{M}_{cv}(\mathbf{k})$ between π bands is zero because these bands are odd under the operation $\{\sigma_h|0\}$. Indicating with $\epsilon_{2\parallel}$ the dielectric function for light polarized parallel to the z axis, we can then write for transition between π bands

$$\epsilon_{2\parallel}(\omega) = 0. \quad (5-30)$$

If the polarization vector \mathbf{e} is perpendicular to the z axis we can take $\mathbf{e}_{\perp} \cdot \mathbf{M}_{cv}(\mathbf{k})$ as independent of \mathbf{k} and we have

$$\begin{aligned} \epsilon_{2\perp}^{(\omega)} &= \frac{2e^2}{cm^2} \frac{1}{\omega^2} |\mathbf{e}_{\perp} \cdot \mathbf{M}_{cv}|^2 \int_{\text{BZ}} \delta(E_c(k_x, k_y) - E_v(k_x, k_y) - \hbar\omega) dk_x dk_y \\ &= \frac{4\pi^2 e^2}{m^2} \frac{1}{\omega^2} |\mathbf{e}_{\perp} \cdot \mathbf{M}_{cv}|^2 J_{cv}(\hbar\omega), \end{aligned} \quad (5-31)$$

where J_{cv} is the expression (5-28). This quantity has been computed numerically by sampling the Brillouin zone in a large number of points, calculating at each point the energy difference $E_c(k_x, k_y) - E_v(k_x, k_y)$, and determining the relative number of states within a suitable energy range. Because of symmetry, only the points of the restricted zone inside the first Brillouin zone have to be considered provided that a weight factor $h/h_{\mathbf{k}}$ (h order of the lattice point group, $h_{\mathbf{k}}$ order of the small point group of \mathbf{k}) is introduced. The triangle ΓPQ shown in Fig. 4-10 was divided into 50,000 points, more than sufficient to give accurate values of the joint density of states. We give in Fig. 5-3 the joint density of states for π bands.^[7] We notice that the saddle point Q is responsible for the sharp peak at $\simeq 4.5$ eV. The point Γ is a maximum and gives a step function. The point P is a minimum, but, because of degeneracy, linear terms in \mathbf{k} in the expansion of the energy difference do not vanish, and the density of states is continuous. In Fig. 5-3 we also give the dielectric function $\epsilon_{2\perp}$ and its experimental values as given by Taft and Philipp.^[8] We notice the satisfactory agreement between theoretical and experimental results in the frequency range from 0 to about 6 eV, which is the region of π band transitions.

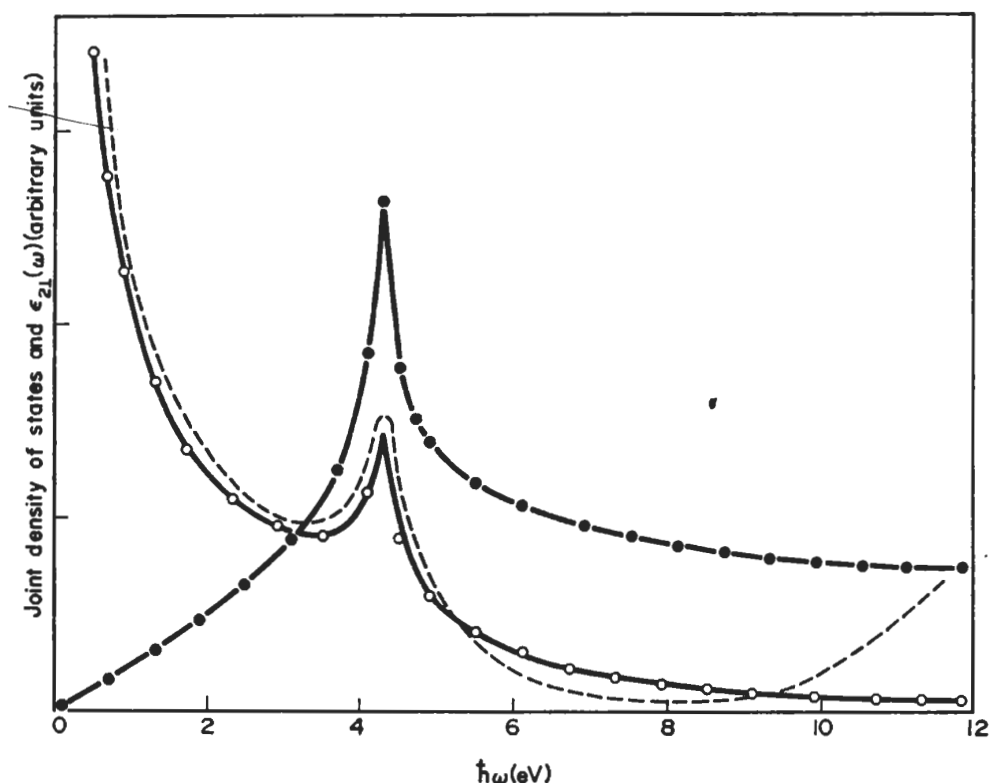


FIG. 5-3. Joint density of states (solid circles) and imaginary part of the dielectric constant (open circles) computed from the π bands of two-dimensional graphite. The experimental dielectric function of Taft and Philipp^[8] is also given. (From Bassani and Pastori Parravicini, ref. [7].)

The contribution to the optical constants from other bands can be dealt with in a similar way.^[7] In general, saddle points are responsible for sharp peaks in the frequency dependence of the imaginary part of the dielectric function as discussed in the preceding sections. It has been shown in this way that the peak at ≈ 14 eV is due to the saddle point at Q for the transition between σ bands. It has also been possible to interpret the structure in $\epsilon_{2||}$ as due to transitions between π bands and σ bands which are allowed for polarization of the electric field in the direction of the c axis.

Experimentally the dielectric function $\epsilon_{2\perp}(\omega)$ has been obtained up to ≈ 25 eV by normal incidence reflectance with the polarization vector of the electric field perpendicular to the z axis.^[8] Different experimental procedures have to be applied to determine $\epsilon_{2||}$ because of the impossibility of growing samples sufficiently thick in the z direction. A first procedure consists in performing reflectivity experiments as function of the angle of incidence and light polarized in the plane of incidence and using the Fresnel relations for anisotropic material.^[9] Another technique consists of analysing electron energy loss data as function of momentum and energy transfer.^[10] The energy loss intensity depends on the values of the dielectric functions both perpendicular and parallel to the c axis, and this allows their determination. It has been proved in this way that $\epsilon_{2||}(\omega)$ is zero for $\hbar\omega < 6$ eV and exhibits two peaks at ≈ 11 and 16 eV.^[10] This result indicates that the separation between σ and π bands is about 6 eV. Furthermore, the positions of the peaks correspond fairly well to the only allowed transitions $Q_{1\sigma}^+ \rightarrow Q_{2\pi}^-$ and $Q_{1\pi}^+ \rightarrow Q_{2\sigma}^-$ at the saddle point Q between σ and π bands, as can be seen from Fig. 4-11.

5-3 Multiphoton transitions

The experimental availability of very intense monochromatic sources has made it possible to detect processes in which two (or more) quanta are simultaneously involved in an electronic transition. The theoretical probability of two quanta processes is in practical experimental situations several orders of magnitude lower than that of single quantum processes, and consequently the detection of two-photon processes can be conveniently realized in a situation in which one-photon processes are not possible. In typical two-photon spectroscopy experiments the two light sources are, firstly, a very intense laser light with fixed frequency, and, secondly, an ordinary light whose frequency can be changed with continuity. The absorption coefficient for ordinary light as a function of frequency is measured when the laser beam is present. As lasers of variable frequency become available, more accurate experiments will be possible by using two or more laser sources, so that the field of multiphoton spectroscopy is likely to develop.

The possibility for a two-photon absorption process was first discussed theoretically by Göppert-Mayer^[11] (1931), but only with the development of laser light was the effect detected experimentally.^[12] Braunstein^[13] calculated the two-photon absorption coefficient in a simplified model semiconductor consisting of a valence, a conduction, and a virtual band. Loudon^[14] gave a more general treatment, and Inoue and Toyozawa^[15] discussed the dependence of the two-photon absorption coefficient on the polarization of the beams.

We wish here to discuss the optical constants in the presence of two radiation beams of frequency ω_1 and ω_2 , with N_1 and N_2 photons per unit volume. In this situation the perturbation term of Section 5-1 b has the form $\mathcal{L}_1 e^{\mp i\omega_1 t} + \mathcal{L}_2 e^{\mp i\omega_2 t}$; to second order the transition probability rate is of type (5-3) with matrix elements containing one or the other of the two terms \mathcal{L}_1 or \mathcal{L}_2 , each with a corresponding argument in the δ function. A first contribution to second order probability rate is the absorption or emission of two photons $\hbar\omega_1$; another is the absorption or emission of two photons $\hbar\omega_2$, but the most important contribution involves one photon $\hbar\omega_1$ and one photon $\hbar\omega_2$. We treat explicitly this last case, pointing out that the others could be dealt with along similar lines. We select the photon energies $\hbar\omega_1$ and $\hbar\omega_2$ such that each one is less, but the sum $\hbar\omega_1 + \hbar\omega_2$ is larger than the energy gap. We can choose the vector potentials $A_1(\mathbf{r}, t)$ and $A_2(\mathbf{r}, t)$ of the radiation beams to be polarized in the fixed direction \mathbf{e}_1 and \mathbf{e}_2

$$A_1(\mathbf{r}, t) = A_{01} \mathbf{e}_1 e^{i(\boldsymbol{\eta}_1 \cdot \mathbf{r} - \omega_1 t)} + \text{c.c.}$$

and

$$A_2(\mathbf{r}, t) = A_{02} \mathbf{e}_2 e^{i(\boldsymbol{\eta}_2 \cdot \mathbf{r} - \omega_2 t)} + \text{c.c.}$$

We describe only absorption processes, and we shall invoke the dipole approximation by letting $\boldsymbol{\eta}_1 = \boldsymbol{\eta}_2 = 0$.

In this approximation we may still consistently disregard the term A^2 in the perturbing Hamiltonian because it does not depend on space and gives no contribution to the matrix elements. The effect of this term in higher order approximations has been considered,^[16] but it is much smaller than the dipole effects which we are going to calculate.

Following Braunstein's procedure,^[13] we consider for simplicity a model semiconductor with a valence band v , a conduction band c , and a typical intermediate

band β (also called virtual band), which is supposed to give most of the contribution to the second order transition probability (5-3). Using the same analysis which leads to (5-9a) but considering two perturbation terms of the type (5-1), we find that the probability per unit time for a transition from the state ψ_{vks} to the state ψ_{cks} , considering as intermediate state $\psi_{\beta ks}$, is

$$\mathcal{P}_{vks \rightarrow cks} = \frac{2\pi}{\hbar} \left(\frac{eA_{01}}{mc} \right)^2 \left(\frac{eA_{02}}{mc} \right)^2 \left| \frac{\mathbf{e}_2 \cdot \mathbf{M}_{c\beta}(\mathbf{k}) \mathbf{e}_1 \cdot \mathbf{M}_{\beta v}(\mathbf{k})}{E_{\beta}(\mathbf{k}) - E_v(\mathbf{k}) - \hbar\omega_1} + \frac{\mathbf{e}_1 \cdot \mathbf{M}_{c\beta}(\mathbf{k}) \mathbf{e}_2 \cdot \mathbf{M}_{\beta v}(\mathbf{k})}{E_{\beta}(\mathbf{k}) - E_v(\mathbf{k}) - \hbar\omega_2} \right|^2 \delta(E_c(\mathbf{k}) - E_v(\mathbf{k}) - \hbar\omega_1 - \hbar\omega_2), \quad (5-32)$$

where

$$\left. \begin{aligned} \mathbf{M}_{\beta v} &= \langle \psi_{\beta}(\mathbf{k}, \mathbf{r}) | \mathbf{p} | \psi_v(\mathbf{k}, \mathbf{r}) \rangle, \\ \mathbf{M}_{c\beta} &= \langle \psi_c(\mathbf{k}, \mathbf{r}) | \mathbf{p} | \psi_{\beta}(\mathbf{k}, \mathbf{r}) \rangle. \end{aligned} \right\} \quad (5-33)$$

As shown in Section 5-1, it is a simple matter to obtain the absorption coefficient for photons of energy $\hbar\omega_1$ in the presence of N_2 photons per unit volume of energy $\hbar\omega_2$ from the transition probability (5-32). We obtain the expression

$$\alpha(\omega_1) = \frac{8\pi^3 \hbar e^2 N_2}{cm^4 n_1 n_2^2 \omega_1 \omega_2} \int_{\text{BZ}} \frac{2d^3\mathbf{k}}{(2\pi)^3} \left| \frac{\mathbf{e}_2 \cdot \mathbf{M}_{c\beta}(\mathbf{k}) \mathbf{e}_1 \cdot \mathbf{M}_{\beta v}(\mathbf{k})}{E_{\beta}(\mathbf{k}) - E_v(\mathbf{k}) - \hbar\omega_1} + \frac{\mathbf{e}_1 \cdot \mathbf{M}_{c\beta}(\mathbf{k}) \mathbf{e}_2 \cdot \mathbf{M}_{\beta v}(\mathbf{k})}{E_{\beta}(\mathbf{k}) - E_v(\mathbf{k}) - \hbar\omega_2} \right|^2 \delta(E_c(\mathbf{k}) - E_v(\mathbf{k}) - \hbar\omega_1 - \hbar\omega_2), \quad (5-34)$$

where n_1 and n_2 are the refractive indices at the two frequencies; the other symbols have already been explained. In deriving (5-34) use has been made of the relation

$$\frac{n_2^2 A_{02}^2 \omega_2^2}{2\pi c^2} = N_2 \hbar\omega_2,$$

which connects the energy density $(n^2 E^2)/4\pi$ of the classical electromagnetic theory with the number of photons per unit volume.

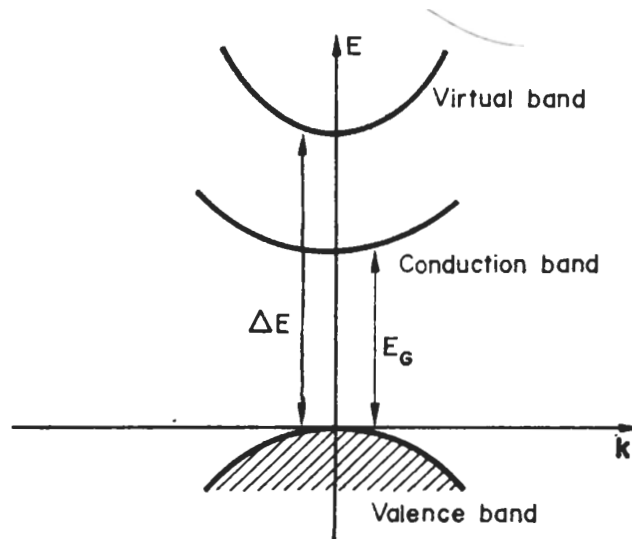


FIG. 5-4. Model semiconductor band structure to calculate two-photon absorption.

The expression (5-34) we can evaluate analytically without difficulty if we make the further approximation that the valence, conduction, and virtual bands are all spherical bands as exemplified in Fig. 5-4. In such a case we can write

$$E_v(\mathbf{k}) = -\gamma_v \frac{\hbar^2}{2m} k^2,$$

$$E_\beta(\mathbf{k}) = \gamma_\beta \frac{\hbar^2}{2m} k^2 + \Delta E,$$

$$E_c(\mathbf{k}) = \gamma_c \frac{\hbar^2}{2m} k^2 + E_G,$$

where ΔE and E_G are shown in Fig. 5-4 and γ_i is a positive number which denotes the inverse of the effective mass in units of m . In the case of allowed transition (i.e. in the case when the matrix elements (5-33) do not vanish because of symmetry), we neglect in (5-34) the smooth dependence of the matrix elements from \mathbf{k} . We can then integrate expression (5-34) neglecting the mixed term and obtain the expression

$$\alpha(\omega_1) = \frac{2^{3/2} \pi e^4 |\mathbf{M}_{c\beta}|^2 |\mathbf{M}_{\beta v}|^2 N_2}{\hbar^2 c m^{3/2} (\gamma_c + \gamma_v)^{3/2} \omega_1 \omega_2} \left(\frac{1}{B} + \frac{1}{C} \right) (\hbar\omega_1 + \hbar\omega_2 - E_G)^{1/2} \quad (5-35a)$$

where

$$B = \left[\Delta E + \frac{\gamma_\beta + \gamma_v}{\gamma_c + \gamma_v} (\hbar\omega_1 + \hbar\omega_2 - E_G) - \hbar\omega_1 \right]^2, \quad (5-35b)$$

$$C = \left[\Delta E + \frac{\gamma_\beta + \gamma_v}{\gamma_c + \gamma_v} (\hbar\omega_1 + \hbar\omega_2 - E_G) - \hbar\omega_2 \right]^2. \quad (5-35c)$$

The value of $\alpha(\omega_1)$ given by (5-35) is in practical experimental situations several orders of magnitude smaller than that obtained for one-photon processes at the critical point M_0 , but it can exhibit a much sharper behaviour just above the energy threshold because expression B and C can become very small.

Braunstein's procedure^[13] has been extended by Bassani and Hassan^[17] to all the different types of critical points discussed in Section 5-2. For two-photon processes it turns out that singularities in the optical constants appear at all critical points and are sharper than those obtained for one-photon processes because of the effect of the energy denominators in the transition probability (5-32). Figure 5-5 shows a typical diagram of optical constants for a two-photon process in the vicinity of a critical point M_1 .

In general, new basic information can be obtained by two-photon spectroscopy because the selection rules for such optical transitions differ from those for one-photon processes. In fact, from (5-33) we see that the allowed transitions in two-photon spectroscopy are those for which matrix elements of the appropriate components of the operator \mathbf{p} between valence virtual states and between virtual conduction states can be simultaneously different from zero. In a crystal with complete cubic symmetry, for example, the only matrix elements different from zero at Γ from an initial state of symmetry Γ_1 are those to states of symmetry Γ_{15} , and from states Γ_{15} to states of symmetry Γ_1 , Γ_{12} , Γ'_{15} or Γ'_{25} (as can be seen from Table 2-18). We therefore have

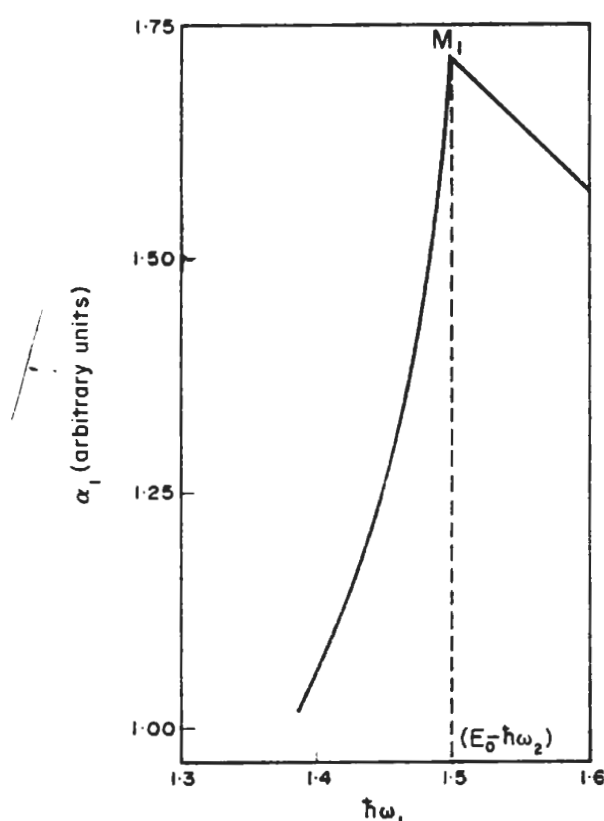


FIG. 5-5. Two-photon absorption coefficient as a function of $\hbar\omega_1$, near a saddle point M_1 . The energy of the critical point is E_0 and the fixed laser frequency is ω_2 . (From A. R. HASSAN, *Nuovo Cimento* **70B**, 21 (1970).)

the result that from a state Γ_1 two-photon transitions are allowed only to states of symmetry Γ_1 , Γ_{12} , Γ'_{15} , or Γ'_{25} and one-photon transitions are allowed only to states of symmetry Γ_{15} .

For all crystals which possess inversion symmetry, a particularly important selection rule is valid at the point Γ ($\mathbf{k} = 0$) and at those symmetry points which contain inversion symmetry since the irreducible representations can be classified as even or odd with respect to inversion. Whilst the allowed transitions in one-photon processes are amongst states with opposite parity, the allowed transitions in two-photon processes are amongst states with the same parity since the intermediate states must have opposite parity to initial and final states. In this situation, the one-photon and two-photon absorption processes are complementary tools for the investigation of the optical properties.

Another important selection rule of general character appears at any \mathbf{k} vector in layer type crystals such as those described in Section 4-2. With light polarized perpendicular (parallel) to the z axis, one-photon transitions are allowed only amongst states of the same (opposite) parity with respect to σ_h as we have discussed in Section 5-2b. Two-photon transitions with both photons polarized perpendicular or parallel to the z axis are allowed only amongst states of the same parity with respect to σ_h . If the two beams have different polarization with respect to the z axis, the allowed transitions are only those amongst states of opposite parity.

So far the experimental results obtained in semiconductors with two-photon spectroscopy^[12] have been mainly limited to cubic crystals without inversion symmetry and the power of the general selection rules described above has not been fully exploited. It is of interest to observe that two-photon spectroscopy may reveal the presence of saddle points in the electronic structure which could not be seen in the usual spectroscopy because they are forbidden to first order.

Theoretical results have been obtained in a similar way also for three-photon transitions by Bassani and Hassan,^[17] and preliminary experimental evidence for three-photon transitions has been obtained in CdS by Catalano *et al.*^[18] We do not wish to discuss these points any further because this field is in its infancy at present, and detailed discussions will have to be left to a later time.

5-4 Indirect band-to-band transitions

5-4a General remarks and electron-phonon interaction

In the previous sections we have considered the interaction of the electrons with the radiation field and we have shown that only vertical transitions may occur. As indicated in Chapter 4, there are a number of crystals, such as semiconductors silicon, germanium, etc., and insulators like AgCl whose electronic structure is characterized by the fact that the bottom of the conduction band and the top of the valence band are at different points of the Brillouin zone. Optical transitions between valence and conduction extrema would be forbidden in this case by momentum conservation (see Section 5-1). Such transitions are experimentally observed, however, albeit they are much weaker than the direct transitions.

Transitions between states which are not vertical in an energy band diagram are called indirect transitions. The possibility of indirect transitions is due to the interaction of the electrons with the vibrations of the lattice. The theory was first provided by Bardeen *et al.*^[19] in order to explain the absorption tail of germanium.

It is well known that one can show by means of canonical transformations^[20] that the Hamiltonian (3-9) describing the motion of the nuclei in the adiabatic approximation is equivalent to the Hamiltonian of a system of independent harmonic oscillators when the total potential energy is expanded up to second order in the nuclear displacements from the equilibrium position and normal coordinates are introduced. Corresponding to every normal mode of wave vector \mathbf{q} there is an harmonic oscillator whose energy can change by integer multiples of $\hbar\omega_{\mathbf{q}}$. The frequency $\omega_{\mathbf{q}}$ as a function of momentum gives the classical vibrational dispersion spectrum, and the quanta $\hbar\omega_{\mathbf{q}}$, by analogy with the photons of the electromagnetic field, are called phonons. At a given \mathbf{q} vector of the Brillouin zone the phonon states can be classified according to the irreducible representations of the group of the vector \mathbf{q} , and their number is given by the number of degrees of freedom of the atoms in the unit cell.

Even in the adiabatic approximation, the presence of the phonon field produces an electron-lattice interaction.^[20] In fact, during the vibrations of the lattice the atoms are displaced from their regular lattice positions, and the actual potential on any electron is consequently changed. To illustrate typical consequences of electron-lattice interaction, we consider a simplified model in which the electron crystal potential is taken

as a sum of superimposed atomic-like potentials rigidly following the displacements of the nuclei. In the above approximation the electron-lattice perturbation Hamiltonian H_{eL} can be written as

$$H_{eL} = \sum_{\mathbf{R}_a} [V(\mathbf{r} - \mathbf{R}_a - \delta\mathbf{R}_a) - V(\mathbf{r} - \mathbf{R}_a)], \quad (5-36)$$

where the sum runs on all the equilibrium atomic positions \mathbf{R}_a in the crystal, $\delta\mathbf{R}_a$ represents the vibrational displacement, and $V(\mathbf{r} - \mathbf{R}_a)$ is the atomic-like potential corresponding to the atom based at \mathbf{R}_a . We expand (5-36) in terms of $\delta\mathbf{R}_a$ and retain the first order term

$$H_{eL} = - \sum_{\mathbf{R}_a} \delta\mathbf{R}_a \cdot \nabla_{\mathbf{r}} V(\mathbf{r} - \mathbf{R}_a). \quad (5-37)$$

It is convenient to expand $\delta\mathbf{R}_a$ in normal coordinates, which is always possible because of the translational symmetry of the lattice. The electron-lattice interaction (5-37) can therefore be separated into a sum of terms, each appropriate to a given phonon of a given branch, of the type

$$H_{ep} = \left(\frac{\hbar}{2M\omega_q} \right)^{1/2} \left[A(\mathbf{q}) \sum_{\mathbf{R}_a} \mathbf{e}_a e^{i(\mathbf{q} \cdot \mathbf{R}_a - \omega_q t)} \cdot \nabla_{\mathbf{r}} V(\mathbf{r} - \mathbf{R}_a) + \text{c.c.} \right], \quad (5-38)$$

where \mathbf{e}_a is an appropriate polarization vector corresponding to a phonon of momentum \mathbf{q} and frequency ω , M indicates the total mass of the crystal, and $A(\mathbf{q})$ and $A^*(\mathbf{q})$ are the annihilation and creation operators respectively. The normalization factor $(\hbar/2M\omega)^{1/2}$ has been introduced so that the matrix elements of $A(\mathbf{q})$ and $A^*(\mathbf{q})$ between multiphonon wave functions satisfy the condition^[20]

$$\left. \begin{aligned} \langle n-1 | A(\mathbf{q}) | n \rangle &= \sqrt{n}, \\ \langle n+1 | A^*(\mathbf{q}) | n \rangle &= \sqrt{(n+1)}, \end{aligned} \right\} \quad (5-39)$$

where $|n\rangle$ indicates a state with phonon occupation number n . The electron-phonon interaction term (5-38) can be rewritten as

$$H_{ep} = A(\mathbf{q}) e^{-i\omega_q t} V_p(\mathbf{q}, \mathbf{r}) + \text{c.c.} \quad (5-40a)$$

with

$$V_p(\mathbf{q}, \mathbf{r}) = \left(\frac{\hbar}{2M\omega_q} \right)^{1/2} \sum_{\mathbf{R}_a} e^{i\mathbf{q} \cdot \mathbf{R}_a} \mathbf{e}_a \cdot \nabla_{\mathbf{r}} V(\mathbf{r} - \mathbf{R}_a). \quad (5-40b)$$

We notice that (5-40b) is a Bloch function of vector \mathbf{q} . When crystal symmetry is fully exploited, $V_p(\mathbf{q}, \mathbf{r})$ belongs to an appropriate irreducible representation of the vector \mathbf{q} as explained in the footnote of Section 3-2c. The first term in (5-40a) produces absorption of a phonon, and the second produces emission of the same phonon.

The theory of indirect optical transitions can now be developed by considering the perturbation Hamiltonian

$$H' = H_{eR} + H_{ep} \quad (5-41)$$

and using the results of second order time dependent perturbation theory summarized by formula (5-3). We obtain all possible expressions of the type (5-3), where one of the matrix elements relates to the electron-radiation interaction and the other to the electron-phonon interaction of the perturbation (5-41). This is because the matrix element of H_{eR} conserves momentum, while the matrix element of H_{ep} transfers a specific momentum \mathbf{q} .

ELECTRONIC STATES AND OPTICAL TRANSITIONS

5-4b Properties of indirect transitions

We wish now to discuss further the absorption coefficient in a model semiconductor with energy bands exemplified by Fig. 5-6. The transition probability per unit time of a process in which the valence electron $\psi_{v\mathbf{k}_1s}$ is scattered to the conduction state $\psi_{c\mathbf{k}_2s}$ and a photon of energy $\hbar\omega$ and a phonon of momentum $\mathbf{q} = \mathbf{k}_2 - \mathbf{k}_1$ (and energy $\hbar\omega_{\mathbf{q}}$) are both absorbed can be obtained from eq. (5-3) as

$$\mathcal{P}_{v\mathbf{k}_1s \rightarrow c\mathbf{k}_2s} = \frac{2\pi}{\hbar} \left(\frac{eA_0}{mc} \right)^2 \left| \frac{\langle \psi_{c\mathbf{k}_2} | V_p(\mathbf{q}, \mathbf{r}) | \psi_{v\mathbf{k}_1} \rangle n_{\mathbf{q}}^{1/2} \langle \psi_{v\mathbf{k}_1} | \mathbf{e} \cdot \mathbf{p} | \psi_{v\mathbf{k}_1} \rangle}{E_c(\mathbf{k}_2) - E_v(\mathbf{k}_1) - \hbar\omega} \right|^2 \times \delta(E_c(\mathbf{k}_2) - E_v(\mathbf{k}_1) - \hbar\omega + \hbar\omega_{\mathbf{q}}). \quad (5-42)$$

UNIVERSITÄT
FEDERALE
ECONOMIQUE
CH-1015
Tél. 021-47 11 11

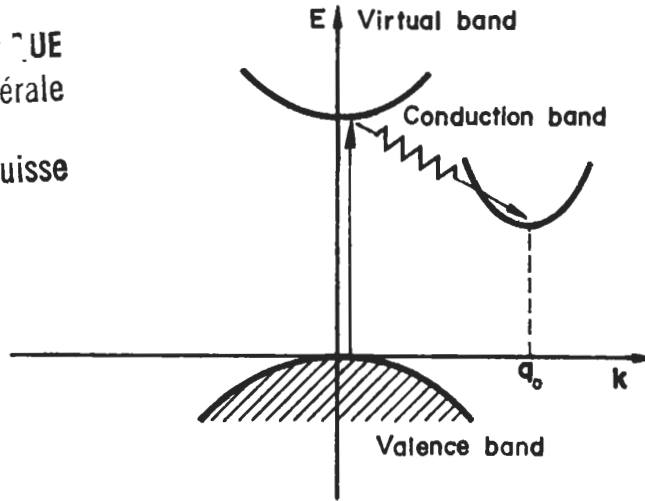


FIG. 5-6. Model semiconductor band structure to calculate the absorption coefficient due to indirect transitions.

In this model we have considered only one virtual band, but it would be easy to add other similar terms associated with other virtual states. In (5-42) $n_{\mathbf{q}}$ denotes the phonon occupation number, which in thermal equilibrium is given by the Bose-Einstein expression

$$n_{\mathbf{q}} = \frac{1}{e^{(\hbar\omega_{\mathbf{q}}/kT)} - 1}.$$

Using the standard procedures of Section 5-1 we obtain the following expression for the absorption coefficient:

$$\alpha_{\text{phonon abs}}(\omega) = \frac{4\pi^2 e^2}{n c m^2 \omega} \int_{\text{BZ}} \int_{\text{BZ}} \frac{2}{(2\pi)^3 (2\pi)^3} d\mathbf{k}_1 d\mathbf{k}_2 \times \left| \frac{\langle \psi_{c\mathbf{k}_2} | V_p(\mathbf{q}, \mathbf{r}) | \psi_{v\mathbf{k}_1} \rangle n_{\mathbf{q}}^{1/2} \langle \psi_{v\mathbf{k}_1} | \mathbf{e} \cdot \mathbf{p} | \psi_{v\mathbf{k}_1} \rangle}{E_c(\mathbf{k}_2) - E_v(\mathbf{k}_1) - \hbar\omega} \right|^2 \delta(E_c(\mathbf{k}_2) - E_v(\mathbf{k}_1) - \hbar\omega + \hbar\omega_{\mathbf{q}}). \quad (5-43)$$

As an example of the application of (5-43) we consider the case of indirect optical transitions between spherical bands. Furthermore, we suppose that the quantity

$$C = \left| \frac{\langle \psi_{c\mathbf{k}_2} | V_p(\mathbf{q}, \mathbf{r}) | \psi_{v\mathbf{k}_1} \rangle \langle \psi_{v\mathbf{k}_1} | \mathbf{e} \cdot \mathbf{p} | \psi_{v\mathbf{k}_1} \rangle}{E_c(\mathbf{k}_1) - E_v(\mathbf{k}_1) - \hbar\omega} \right|^2$$

to a good degree of approximation can be regarded as independent of the wave vectors \mathbf{k}_1 and \mathbf{k}_2 in the vicinity of the extrema; this is a good approximation for allowed transitions when the energy denominator in (5-43) is not too small. The absorption of light begins at $\hbar\omega = E_G - k\theta$, where E_G is the energy gap and $k\theta$ is the energy of the phonon with vector \mathbf{q}_0 equal to the vector which connects band extrema in the Brillouin zone. For phonon energies $\hbar\omega$ a little larger than $E_G - k\theta$, transitions involve pairs of valence and conduction states separated in momentum space by vectors very near to \mathbf{q}_0 so that it is a good approximation to take the energy of the phonon involved as a constant equal to $k\theta$ and to maintain the phonon occupation number $n_{\mathbf{q}}$ independent of \mathbf{k}_1 and \mathbf{k}_2 . The expression (5-43) then becomes

$$\alpha_{\text{phonon abs}}(\omega) = \frac{4\pi^2 e^2 C n_{\mathbf{q}_0}}{n c m^2 \omega} \int_{\text{BZ}} \int_{\text{BZ}} \frac{2}{(2\pi)^3 (2\pi)^3} d\mathbf{k}_1 d\mathbf{k}_2 \delta(E_c(\mathbf{k}_2) - E_v(\mathbf{k}_1) - \hbar\omega + k\theta). \quad (5-44)$$

In the case of the parabolic bands, we can write

$$E_c(\mathbf{k}_2) = \frac{\hbar^2 \mathbf{k}_2^2}{2m_c^*} + E_G \quad \text{and} \quad E_v(\mathbf{k}_1) = -\frac{\hbar^2 \mathbf{k}_1^2}{2m_v^*},$$

where \mathbf{k}_1 and \mathbf{k}_2 are referred to their respective extrema. If we introduce the above expression into (5-44), use polar coordinates, and perform the integrations by means of property (5-22), we obtain

$$\begin{aligned} & \int_{\text{BZ}} \int_{\text{BZ}} \frac{2}{(2\pi)^3 (2\pi)^3} d\mathbf{k}_1 d\mathbf{k}_2 \delta\left(\frac{\hbar^2 \mathbf{k}_2^2}{2m_c^*} + \frac{\hbar^2 \mathbf{k}_1^2}{2m_v^*} + E_G - \hbar\omega + k\theta\right) \\ &= \begin{cases} 0 & \text{for } \hbar\omega < E_G - k\theta \\ \frac{1}{8(2\pi)^3} \left(\frac{2m_v^*}{\hbar^2}\right)^{3/2} \left(\frac{2m_c^*}{\hbar^2}\right)^{3/2} (\hbar\omega - E_G + k\theta)^2 & \text{for } \hbar\omega > E_G - k\theta. \end{cases} \end{aligned}$$

Substituting the above expression into (5-44) we find that the contribution to the absorption coefficient due to the absorption of a phonon is given by

$$\alpha_{\text{phonon abs}}(\omega) = \begin{cases} 0 & \text{for } \hbar\omega < E_G - k\theta, \\ C_1 (\hbar\omega - E_G + k\theta)^2 n_{\mathbf{q}_0} & \text{for } \hbar\omega > E_G - k\theta, \end{cases} \quad (5-45a)$$

where

$$C_1 = \frac{C}{\omega} \frac{4\pi^2 e^2}{n c m^2} \frac{1}{8(2\pi)^3} \left(\frac{2m_v^*}{\hbar^2}\right)^{3/2} \left(\frac{2m_c^*}{\hbar^2}\right)^{3/2}. \quad (5-45b)$$

Another contribution to the absorption coefficient is due to the emission of a phonon and can be obtained using the same procedure, the only differences from the previous case being the sign of the phonon energy and the normalization (5-39). We obtain

$$\alpha_{\text{phonon emiss}}(\omega) = \begin{cases} 0 & \text{for } \hbar\omega < E_G + k\theta, \\ C_1 (\hbar\omega - E_G - k\theta)^2 (n_{\mathbf{q}_0} + 1) & \text{for } \hbar\omega > E_G + k\theta, \end{cases} \quad (5-46)$$

as the contribution to indirect transitions due to creation of a phonon of momentum \mathbf{q}_0 .

The total absorption coefficient is then

$$\alpha_{\text{tot}}(\omega) = \alpha_{\text{phonon abs}}(\omega) + \alpha_{\text{phonon emiss}}(\omega), \quad (5-47)$$

which depends quadratically on energy and exhibits two steps—one for $\hbar\omega = E_G - k\theta$ and one for $\hbar\omega = E_G + k\theta$, the difference between the two steps being equal to $2k\theta$. We should like to point out that indirect transitions have a strong temperature dependence because of n_{q_0} ; at very low temperature only the contribution $\alpha_{\text{phonon emiss}}$ can be observed but, increasing the temperature, the contribution $\alpha_{\text{phonon abs}}$ comes in with relative intensity given by the Boltzman factor. One should note that at a given q_0 more phonons can participate in optical transitions, each of them giving a contribution to the absorption coefficient in accordance with (5-45) and (5-46).

Selection rules play a role in determining which phonon contribute to indirect transitions. The allowed transitions are those for which the matrix elements of the appropriate component of the operator \mathbf{p} , and the matrix element of the operator $V_p(\mathbf{q}, \mathbf{r})$ with the symmetry of the phonon in consideration between virtual states and initial or final states can be simultaneously different from zero. Using the results of Section 2-4, selection rules for indirect transitions can easily be established. They have been used by Lax and Hopfield^[21] to locate the type of phonon which participate in the absorption edge of germanium and silicon and by a number of authors for other compounds.^[22]

In conclusion it is worth-while to mention that the theory of indirect transitions has been extended to third order to include the cases of two-phonon one-photon transitions and two-photon phonon-assisted transitions.^[23] In particular, Bassani and Hassan^[23] have shown that the probability of two-photon one-phonon transitions is much higher than the probability of three-photon transitions with the intensity of the light sources presently available. In a similar way, one-photon one-phonon transitions are much more probable than two-photon transitions, and for this reason we have attributed the absorption of a typical semiconductor sketched in Fig. 5-6 to one-photon phonon-assisted transitions.

APPENDIX 5A

Matrix elements of one-electron and two-electron operators between determinantal states

In this and the following chapter we need matrix elements of one-electron and two-electron operators between Slater determinantal states.^[24] We summarize here some results which are useful in their calculation.

Let $|A\rangle$ be the determinantal state

$$|A\rangle = \mathcal{A}\{a_1(1) a_2(2) \dots a_N(N)\}$$

for a N particle system, a_i being a set of orthonormal one-electron function and \mathcal{A} the operator of antisymmetrization with the appropriate normalization factor $(N!)^{-1/2}$. Let

$$G_1 = \sum_{i=1}^N g_1(i)$$

be an operator sum of one particle operators and

$$G_2 = \frac{1}{2} \sum_{i \neq j} g_2(i, j)$$

be an operator sum of two-particle operators.

The expectation values of the operators G_1 and G_2 on the state $|A\rangle$ are, respectively,

$$\langle A | G_1 | A \rangle = \sum_i \langle a_i | g_1 | a_i \rangle \quad (5A-1)$$

and

$$\langle A | G_2 | A \rangle = \frac{1}{2} \sum_{ij} [\langle a_i a_j | g_2 | a_i a_j \rangle - \langle a_i a_j | g_2 | a_j a_i \rangle], \quad (5A-2)$$

where the usual abbreviation for two-electron integrals has been used, i.e.

$$\langle a_1 a_2 | g_2 | a_3 a_4 \rangle = \iint a_1^*(\mathbf{r}_1) a_2^*(\mathbf{r}_2) g_2(\mathbf{r}_1, \mathbf{r}_2) a_3(\mathbf{r}_1) a_4(\mathbf{r}_2) d\mathbf{r}_1 d\mathbf{r}_2.$$

The matrix elements of the operators G_1 and G_2 between the states:

$$|A\rangle = \mathcal{A}\{a_1(1) a_2(2) \dots \underline{a_k(k)} \dots a_N(N)\}$$

and

$$|B\rangle = \mathcal{A}\{a_1(1) a_2(2) \dots \underline{b_k(k)} \dots a_N(N)\},$$

which differ by only one of the one-particle functions, are, respectively,

$$\langle A | G_1 | B \rangle = \langle a_k | g_1 | b_k \rangle \quad (5A-3)$$

and

$$\langle A | G_2 | B \rangle = \sum_j [\langle a_k a_j | g_2 | b_k a_j \rangle - \langle a_k a_j | g_2 | a_j b_k \rangle]. \quad (5A-4)$$

From (5A-1) it follows that

$$\langle B | G_1 | B \rangle - \langle A | G_1 | A \rangle = \langle b_k | g_1 | b_k \rangle - \langle a_k | g_1 | a_k \rangle. \quad (5A-5)$$

From (5A-2) we easily obtain

$$\begin{aligned} \langle B | G_2 | B \rangle - \langle A | G_2 | A \rangle &= \sum_j [\langle b_k a_j | g_2 | b_k a_j \rangle - \langle b_k a_j | g_2 | a_j b_k \rangle] \\ &\quad - [\langle b_k a_k | g_2 | b_k a_k \rangle - \langle b_k a_k | g_2 | a_k b_k \rangle] \\ &\quad - \sum_j [\langle a_k a_j | g_2 | a_k a_j \rangle - \langle a_k a_j | g_2 | a_j a_k \rangle]. \end{aligned} \quad (5A-6)$$

The matrix elements of the operators G_1 and G_2 between the states

$$|A\rangle = \mathcal{A}\{a_1(1) a_2(2) \dots \underline{a_k(k)} \dots \underline{a_l(l)} \dots a_N(N)\}$$

and

$$|C\rangle = \mathcal{A}\{a_1(1) a_2(2) \dots \underline{c_k(k)} \dots \underline{c_l(l)} \dots a_N(N)\}$$

which differ in two one-electron functions, are

$$\langle A | G_1 | C \rangle = 0 \quad (5A-7)$$

and

$$\langle A | G_2 | C \rangle = \langle a_k a_l | g_2 | c_k c_l \rangle - \langle a_k a_l | g_2 | c_l c_k \rangle. \quad (5A-8)$$

The matrix elements of the operators G_1 and G_2 between states which differ by more than two pairs of functions are zero.

APPENDIX 5B

Koopmans' approximation

From Section 3-1 we consider the Hamiltonian for the many-electron system of the form

$$H_e(\mathbf{r}_1, \mathbf{r}_2, \dots, \mathbf{r}_N) = \sum_{i=1}^N H_i + \frac{1}{2} \sum_{i \neq j} \frac{e^2}{r_{ij}} \quad (5B-1)$$

with

$$H_i = -\frac{\hbar^2}{2m} \nabla_i^2 - \sum_I \frac{z_I e^2}{|\mathbf{R}_I - \mathbf{r}_i|}.$$

We write the ground state of the system in the form

$$\Psi_0 = \mathcal{A}\{\psi_1(1), \psi_2(2), \dots, \psi_N(N)\},$$

where the ψ_i satisfy Hartree-Fock equations

$$H_{\text{HF}}\psi_i = E_i\psi_i, \quad (5B-2)$$

where

$$H_{\text{HF}} = H(1) + V_{\text{coul}}(1) + V_{\text{exch}}(1) \quad (5B-3)$$

with

$$V_{\text{coul}}\psi_i(1) = \sum_j \psi_j(1) \int \psi_j^*(2) \frac{e^2}{r_{12}} \psi_j(2) d\tau_2 \quad (5B-4)$$

and

$$V_{\text{exch}}\psi_i = - \sum_j \psi_j(1) \int \psi_j^*(2) \frac{e^2}{r_{12}} \psi_i(2) d\tau_2. \quad (5B-5)$$

In (5B-4) and (5B-5) integration involves also summation over spin coordinates. Multiplying (5B-2) by $\langle \psi_i |$ we have in general for any Hartree-Fock state:

$$E_i = \langle \psi_i | H_i | \psi_i \rangle + \sum_j \left[\langle \psi_i \psi_j | \frac{e^2}{r_{12}} | \psi_i \psi_j \rangle - \langle \psi_i \psi_j | \frac{e^2}{r_{12}} | \psi_j \psi_i \rangle \right]. \quad (5B-6)$$

Consider a trial excited state Φ_{φ_i, ψ_i} obtained by replacing in Ψ_0 one of the function ψ_i with an excited function φ_i , with all other functions unchanged. This corresponds to neglecting dynamical polarization effects. We may thus write

$$\Phi_{\varphi_i, \psi_i} = \mathcal{A}\{\psi_1(1), \psi_2(2), \dots, \varphi_i(i), \dots, \psi_N(N)\}.$$

By using expression (5A-5) and (5A-6),

$$\begin{aligned} & \langle \Phi_{\varphi_i, \psi_i} | H_e | \Phi_{\varphi_i, \psi_i} \rangle - \langle \Psi_0 | H_e | \Psi_0 \rangle \\ &= \langle \varphi_i | H_i | \varphi_i \rangle - \langle \psi_i | H_i | \psi_i \rangle \\ &+ \sum_j \left[\langle \varphi_i \psi_j | \frac{e^2}{r_{12}} | \varphi_i \psi_j \rangle - \langle \varphi_i \psi_j | \frac{e^2}{r_{12}} | \psi_j \varphi_i \rangle \right] \\ &- \left[\langle \varphi_i \psi_i | \frac{e^2}{r_{12}} | \varphi_i \psi_i \rangle - \langle \varphi_i \psi_i | \frac{e^2}{r_{12}} | \psi_i \varphi_i \rangle \right] \\ &- \sum_j \left[\langle \psi_i \psi_j | \frac{e^2}{r_{12}} | \psi_i \psi_j \rangle - \langle \psi_i \psi_j | \frac{e^2}{r_{12}} | \psi_j \psi_i \rangle \right]. \end{aligned} \quad (5B-7)$$

When the excited function φ_i satisfies the Hartree-Fock equation (5B-2) with V_{coul} and V_{exch} defined by (5B-4) and (5B-5), (5B-7) takes the more effective form

$$\begin{aligned} \langle \Phi_{\varphi_i, \psi_i} | H_e | \Phi_{\varphi_i, \psi_i} \rangle - \langle \Psi_0 | H_e | \Psi_0 \rangle \\ = E'_i - E_i - \left[\langle \varphi_i \psi_i | \frac{e^2}{r_{12}} | \varphi_i \psi_i \rangle - \langle \varphi_i \psi_i | \frac{e^2}{r_{12}} | \psi_i \varphi_i \rangle \right], \end{aligned} \quad (5B-8)$$

where use has been made of (5B-6) and of a similar expression for the eigenvalue E'_i of φ_i . In most practical situations in crystals, the electron-hole interaction

$$\left[\langle \varphi_i \psi_i | \frac{e^2}{r_{12}} | \varphi_i \psi_i \rangle - \langle \varphi_i \psi_i | \frac{e^2}{r_{12}} | \psi_i \varphi_i \rangle \right]$$

is negligible compared with the difference $E'_i - E_i$ because the wave functions extend over the entire lattice. In this case we have

$$\langle \Phi_{\varphi_i, \psi_i} | H_e | \Phi_{\varphi_i, \psi_i} \rangle - \langle \Psi_0 | H_e | \Psi_0 \rangle \approx E'_i - E_i, \quad (5B-9)$$

i.e. the difference of the expectation values of the many-body Hamiltonian H_e on two determinantal states which differ by only one of the one-particle functions equals the difference of the corresponding Hartree-Fock eigenvalues (Koopmans' approximation).

With a similar procedure it would be easy to show that the Hartree-Fock energy of each one-electron state coincides with the energy required to remove that electron from the system (Koopmans' theorem), provided that one neglects dynamical polarization effects.

When the Hamiltonian (5B-1) does not contain spin dependent terms and the ground state Ψ_0 has total spin equal zero, it is convenient to take trial excited states of a definite spin multiplicity. For triplet states (total spin = 1) we have:

$$\left. \begin{aligned} &\Phi_{\varphi_{i\frac{1}{2}}, \psi_{i\frac{1}{2}}}, \\ &\frac{1}{\sqrt{2}} (\Phi_{\varphi_{i\frac{1}{2}}, \psi_{i\frac{1}{2}}} - \Phi_{\varphi_{i\frac{1}{2}}, \psi_{i\frac{3}{2}}}), \\ &\Phi_{\varphi_{i\frac{3}{2}}, \psi_{i\frac{1}{2}}}, \end{aligned} \right\} \quad (5B-10)$$

and for singlet states (total spin = 0)

$$\frac{1}{\sqrt{2}} (\Phi_{\varphi_{i\frac{1}{2}}, \psi_{i\frac{1}{2}}} + \Phi_{\varphi_{i\frac{3}{2}}, \psi_{i\frac{3}{2}}}), \quad (5B-11)$$

where $\varphi_{i\frac{1}{2}}$, $\varphi_{i\frac{3}{2}}$ indicates the product $\varphi_i(\mathbf{r})\alpha$, $\varphi_i(\mathbf{r})\beta$ respectively.

We indicate trial excited states of type (5B-10) and (5B-11) of a given spin multiplicity with $\Phi_{\varphi_i, \psi_i}^{(M)}$, where $M = 1$ for triplet states and $M = 0$ for singlet states. With procedures similar to those applied to derive (5B-8),

$$\begin{aligned} \langle \Phi_{\varphi_i, \psi_i}^{(M)} | H_e | \Phi_{\varphi_i, \psi_i}^{(M)} \rangle - \langle \Psi_0 | H_e | \Psi_0 \rangle \\ = E'_i - E_i - \left[\langle \varphi_i \psi_i | \frac{e^2}{r_{12}} | \varphi_i \psi_i \rangle - 2\delta_M \langle \varphi_i \psi_i | \frac{e^2}{r_{12}} | \psi_i \varphi_i \rangle \right], \end{aligned} \quad (5B-12)$$

where $\delta_M = 1$ for singlet states and $\delta_M = 0$ for triplet states, and integration involves only space coordinates. We will use this result in the next chapter in discussing singlet and triplet excitons. In the Koopmans' approximation (5B-12) is replaced by (5B-9).

References and notes

- [1] D. L. GREENAWAY and G. HARBEKE, *Optical Properties and Band Structure of Semiconductors* (Pergamon Press, 1968).
- [2] See, for example, F. BASSANI, in *Proceedings of the International School of Physics "Enrico Fermi"* (Academic Press, 1966), vol. 34, p. 33. For additional information to various problems related to optical transitions, we recommend F. ABELÈS (ed.), *Optical Properties of Solids* (North-Holland, 1972).
- [3] F. STERN, *Solid State Physics* **15**, 300 (1963); J. TAUC, in *Proceedings of the International School of Physics "Enrico Fermi"* (Academic Press, 1966), vol. 34, p. 63.
- [4] For a general analysis of sum rules see M. ALTARELLI, D. L. DEXTER, H. M. NUSSENZVEIG, and D. Y. SMITH, *Phys. Rev. B* **6**, 4502 (1972); M. ALTARELLI and D. Y. SMITH, *Phys. Rev. B* **9**, 1290 (1974).
- [5] J. C. PHILLIPS, *Phys. Rev.* **104**, 1263 (1956); L. VAN HOVE, *Phys. Rev.* **89**, 1189 (1953).
- [6] D. BRUST, J. C. PHILLIPS, and F. BASSANI, *Phys. Rev. Letters* **9**, 94 (1962); D. BRUST, *Phys. Rev.* **134**, A 1337 (1964). See also the review article by J. C. PHILLIPS, *Solid State Physics* **18**, 56 (1966).
- [7] F. BASSANI and G. PASTORI PARRAVICINI, *Nuovo Cimento* **50B**, 95 (1967).
- [8] E. A. TAFT and H. R. PHILIPP, *Phys. Rev.* **138**, A 197 (1965).
- [9] D. L. GREENAWAY, G. HARBEKE, F. BASSANI, and E. TOSATTI, *Phys. Rev.* **178**, 1340 (1969).
- [10] K. ZEPPEFELD, *Phys. Letters* **25A**, 335 (1967); E. TOSATTI, *Nuovo Cimento* **63B**, 54 (1969); E. TOSATTI and F. BASSANI, *Nuovo Cimento* **65B**, 161 (1970).
- [11] M. GÖPPERT-MAYER, *Ann. Phys.* **9**, 273 (1931).
- [12] See, for example: W. KAISER and C. G. B. GARRETT, *Phys. Rev. Letters* **7**, 229 (1961); J. A. GIORDMAINE and J. A. HOWE, *Phys. Rev. Letters* **11**, 207 (1963); I. D. ABELLA, *Phys. Rev. Letters* **9**, 453 (1962); J. J. HOPFIELD, J. M. WORLOCH, and K. PARK, *Phys. Rev. Letters* **11**, 414 (1963); J. J. HOPFIELD and J. M. WORLOCH, *Phys. Rev.* **137**, A 1455 (1965); N. G. BASOV, A. Z. GRASYUK, I. G. ZUBAREV, and V. A. KATULIN, *JETP Letters* **1**, 118 (1965); C. K. N. PATEL, P. A. FLEURY, R. E. SLUSHER and H. L. FRISCH, *Phys. Rev. Letters* **16**, 971 (1966); P. J. REGENSBURGER and E. PANIZZA, *Phys. Rev. Letters* **18**, 113 (1967); E. PANIZZA, *Appl. Phys. Letters* **10**, 265 (1967).
- [13] R. BRAUNSTEIN, *Phys. Rev.* **125**, 475 (1962). See also R. BRAUNSTEIN and M. OCKMAN, *Phys. Rev.* **134A**, 499 (1964).
- [14] R. LOUDON, *Proc. Phys. Soc.* **80**, 952 (1962).
- [15] M. INOUE and Y. TOYOZAWA, *J. Phys. Soc. Japan* **20**, 363 (1965). See also D. FRÖHLICH, B. STAGINNUS, and S. THURM, *Phys. Status Solidi* **40**, 287 (1970).
- [16] M. IANNUZZI and E. POLACCO, *Phys. Rev. Letters* **13**, 371 (1964); M. IANNUZZI and E. POLACCO, *Phys. Rev.* **138**, A 806 (1965); G. FORNACA, M. IANNUZZI, and E. POLACCO, *Nuovo Cimento* **36**, 1230 (1965); A. GOLD and J. P. HERNANDEZ, *Phys. Rev.* **139**, A2002 (1965).
- [17] F. BASSANI and A. R. HASSAN, *Opt. Commun.* **1**, 371 (1970); A. R. HASSAN, *Nuovo Cimento* **70B**, 21 (1970); F. BASSANI and A. R. HASSAN, *Nuovo Cimento* **7B**, 313 (1972).
- [18] I. M. CATALANO, A. CINGOLANI, and A. MINAFRA, *Phys. Rev.* **5B**, 1629 (1972); *Optics Commun.* **5**, 212 (1972).
- [19] J. BARDEEN, F. J. BLATT, and L. J. HALL, in *Photoconductivity Conference* (R. G. BRECKENRIDGE et al., eds.) (Wiley, 1957), p. 146.
- [20] J. M. ZIMAN, *The Principles of the Theory of Solids* (Cambridge University Press, 1972); R. E. PEIERLS, *Quantum Theory of Solids* (Clarendon Press, 1955).
- [21] M. LAX and J. J. HOPFIELD, *Phys. Rev.* **124**, 115 (1961).
- [22] See, for example: F. BASSANI, R. S. KNOX, and W. BEAL FOWLER, *Phys. Rev.* **137**, A 1217 (1965); N. O. FOLLAND and F. BASSANI, *J. Phys. Chem. Solids* **29**, 281 (1968).
- [23] V. A. KOVARSKII and E. V. VITTU, *Soviet Physics Semiconductors* **3**, 354 (1969); B. M. ASHKINADZE, A. I. BODRYSHIVA, E. V. VITTU, V. A. KOVARSKY, A. V. LELYAKOV, S. A. MOSHALENKO, S. L. PYSHKIN, and S. I. RADAUTSAN, in *Proceedings of the IXth International Conference on the Physics of Semiconductors* (Moscow, 1968), p. 189; B. M. ASHKINADZE, S. M. RYVKIN, and I. D. YAROSHETSKII, *Soviet Physics Semiconductors* **2**, 1285 (1969); N. O. FOLLAND, *Phys. Rev.* **1B**, 1648 (1970); F. BASSANI and A. R. HASSAN, *Nuovo Cimento* **7B**, 313 (1972).
- [24] J. C. SLATER, *Phys. Rev.* **34**, 1293 (1929), **38**, 1109 (1931). See also M. TINKHAM, *Group Theory and Quantum Mechanics* (McGraw-Hill, 1964).
- [25] T. KOOPMANS, *Physica* **1**, 104 (1934); F. SEITZ, *The Modern Theory of Solids* (McGraw-Hill, 1940).